Longitudinal Flight Dynamics Modeling and Stability Analysis of the Flapping Wing Aircraft with Folding Wing

Xuejiao Zhang* and Yonghai Wang**
* Beijing Institute of Space Long March Vehicle, CALT, China
No.1 Nandahongmen Road, Fengtai District, Beijing, China and 15901102629@163.com
** Beijing Institute of Space Long March Vehicle, CALT, China
No.1 Nandahongmen Road, Fengtai District, Beijing, China and 1985565518@qq.com

Abstract

Foldable Flapping Wing Aircraft is a kind of aircraft that generates lift and thrust with foldable wings flapping up and down. In this paper, the kinematics model of foldable Flapping Wing Aircraft is constructed with reference to bats. The aerodynamic modeling method is a combination of the quasi-constant model and the elemental theory with wash effect. The longitudinal dynamics model is constructed through multi-rigid body finite element method. Robust variable gain control method is used to analyze the closed-loop longitudinal stability of foldable Flapping Wing Aircraft.
Keywords: Foldable Flapping Wing Aircraft, aerodynamic modeling, flight dynamics modeling, stability analysis

1. Introduction

Flapping Wing Aircraft (abbreviated as FWA) with foldable wing is a kind of aircraft that generates lift and thrust by imitating insects, birds or bats with foldable wings flapping up and down. In recent years, research on bionic FWA has been increasing and various structural forms of FWA have been proposed. The flying environment of the FWA is similar to that of birds or large insects, such as the similar hydrodynamics with low Reynolds number and unsteady aerodynamics[1,2]. During the flight, the kinematic model of the flapping creature usually has four degrees of freedom, flutter, swing, twist and stretch[3]. Thielicke[4] studied the aerodynamic characteristics of birds' armwing and handwing with different cambers and thicknesses during slow flight.

The traditional kinematic model of the bionic FWA only considers two degrees of freedom of flutter and torsion. Based on the traditional FWA kinematic model, this paper adds two new degrees of freedom: in-plane folding and out-of-plane folding. In this paper, the aerodynamic modeling method of four-degree-of-freedom kinematics model is a combination of the quasi-constant model and the elemental theory with wash effect. The longitudinal dynamics model is constructed through multi-rigid body finite element method. The Floquet-Lyapunov Method is used to analyze the open-loop longitudinal stability. Robust variable gain control method is used to analyze the closed-loop longitudinal stability.

2. Construction of kinematic model

2.1 Definition of coordinate system

The definition of relevant coordinate system of the four-degree-of-freedom FWA kinematics model is as follows：
(1) Inertial coordinate system $OXYZ$
In the inertial coordinate system, the origin O coincides with the centroid of the aircraft's departure time. The axis OX is the intersection of the aircraft track surface and the horizontal plane, pointing to the takeoff direction of the aircraft. The axis OY points upward along the vertical line. The OZ axis is perpendicular to the other two axes and forms the right hand coordinate system.
(2) Body coordinate system $oxyz$
The origin o of the Body coordinate system is the instantaneous centroid of the aircraft. The ox axis coincides with the longitudinal axis of the body, pointing to the head of the body；The oy axis is perpendicular to the ox axis and

Xuejiao Zhang, Yonghai Wang

points to the right wing of the body. The oz axis is in the longitudinal symmetry plane of the body, perpendicular to the other two axes and forming a right-handed coordinate system, as shown in Figure 1.
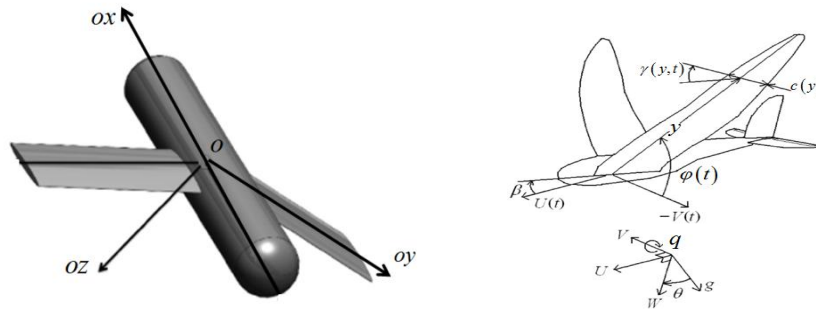

Figure 1: Schematic diagram of Body coordinate system   Figure 2: Parameter definition diagram

2.2 Kinematic model of FWA

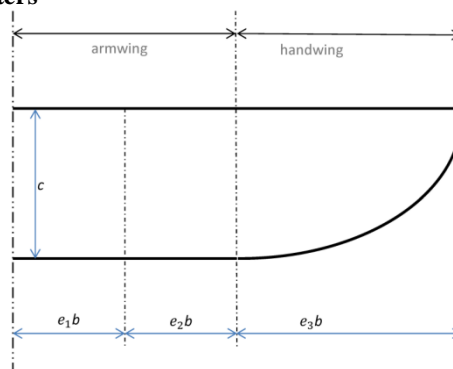**(1)Definition of kinematic parameters**

Figure 3: Geometric schematic of FWA right wing

Explain the geometric characteristics of the wing, with the FWA right wing as an example. b is the half length of the wingspan. c is the chord length at the wing root. The wing is a flat wing type that can be divided into Armwing and Handwing along the spanwise direction. Armwing is a quadrilateral whose length is $e_1 b + e_2 b$, width is c .The shape of Hand wing is a quarter ellipse, whose long semi-axis is $e_3 b$, and the short semi-axis is c , as shown in Figure 2 and Figure 3.

A complete flapping cycle of the wing includes downstroke and upstroke. During the flapping down, the wing is fully deployed with only two degrees of freedom (flutter and twist). The flutter angle $\varphi(t)$ is the angle between the wing plane and the oxy plane. The central axis of the twist angle $\gamma(y,t)$ is the quarter of the wing chord length, as shown in Figure 2. During the flapping up, the kinematic model of wing includes four degrees of freedom (flutter, twist, in-plane folding and out-of-plane folding). In-plane folding angle $\theta_1(t)$ and $\theta_2(t)$ 如 is shown as Figure 4. Out-of-plane folding angle is shown as Figure 5.
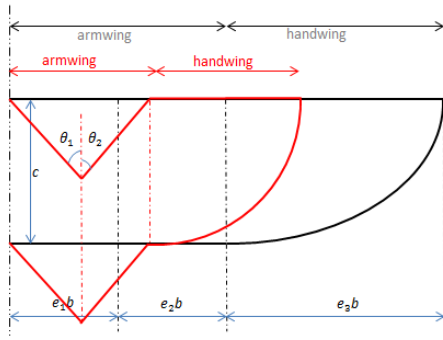
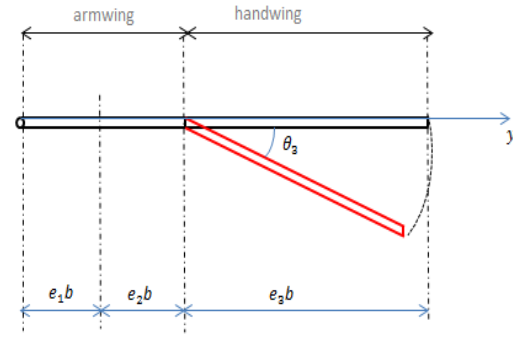Figure 4: In-plane folding diagram   Figure 5: Out-of-plane folding diagram

Note: Figure 4 is the top view of right wing, in which the black solid line corresponds to the full extension of the wing during flapping down, the red solid line indicates the in-plane folding of the wing during flapping up. Figure 5 is the rear view of right wing, the solid black line in the figure indicates that the wing is fully deployed during flapping down, a solid red line indicates that the wing has an out-of-plane fold during flapping up.
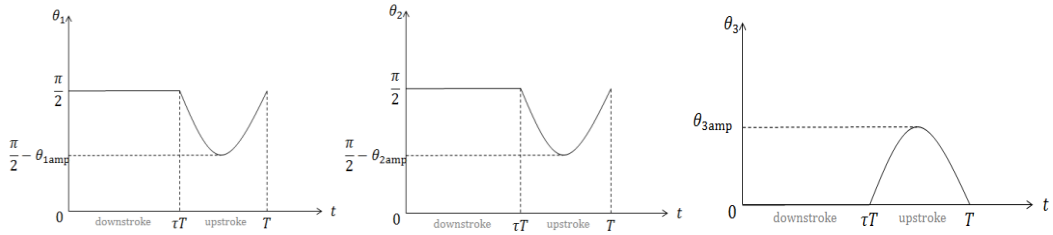
$$T = T_{\text{down}} + T_{\text{up}} \tag{1}$$

$$\tau = \frac{T_{down}}{T}\ (\ \tau \in (0.48, 0.54)\ ) \tag{2}$$

$$b(t) = e_1 b \sin\theta_1(t) + e_2 b \sin\theta_2(t) + e_3 b, t \in (0, T) \tag{3}$$

$$c(y) = \begin{cases} c & , y \in [0, e_1 b] \\ c & , y \in [e_1 b, (e_1 + e_2)b] \\ \sqrt{c^2 - \dfrac{c^2}{(e_3 b)^2}\left[y - (e_1 + e_2)b\right]^2} & , y \in \left[(e_1 + e_2)b, b\right] \end{cases} \tag{4}$$

(2) Kinematic model of foldable wing

(a) In-plane folding angle $\theta_1(t)$ (b) In-plane folding angle $\theta_2(t)$ (c) Out-of-plane folding angle $\theta_3(t)$

Figure 6: Folding angle function curve of foldable wing

The three folding angle functions are trigonometric functions of a half cycle, and the function curve is shown in Figure 6. The expressions of the flutter angle and the twist angle are as follows:

$$\begin{cases} \varphi(t) = \varphi_{\max} \cos(2\pi f t) + \varphi_0 \\ \gamma(y, t) = \dfrac{y}{b}\left[\gamma_{\max} \cos(2\pi f t) + \gamma_0\right] \end{cases} \tag{5}$$

Xuejiao Zhang, Yonghai Wang

In the above formula, $\varphi_{\max}$ is the amplitude of the flutter angle, $\gamma_{\max}$ is the amplitude of the twist angle. φ_0 and γ_0 is the initial flutter angle and the initial twist angle of flapping wing at the equilibrium position. y is the distance from this point to wing root along the spanwise direction. f is flutter frequency. b is the half length of the wingspan. The expression of the twist angle indicates that at a certain moment, the twist angle gradually increases from the wing root to the wing tip and reaches the maximum at the wing tip.

3. Construction of aerodynamic model

3.1 Kinematic model of the tiny wing strip

According to the elemental theory, take a tiny wing strip along the wingspan as a research object. FWA flies forward at a speed of v_∞. The tiny wing strip has three velocity components: forward speed v_∞, flutter linear velocity v_φ and twist linear velocity v_γ. Assuming that the wing is stationary, the airflow makes relative motion to the tiny strip. Take the aerodynamic center of the airfoil (1/4 wing chord) as the reference point and the kinematic model of the strip is shown in Fig. 7. The flutter linear velocity v_φ and twist linear velocity v_γ of the strip are determined as the following:

$$\begin{cases} v_\varphi = -y\dot{\varphi}(t) \\ v_\gamma = -\frac{1}{4}c(y)\dot{\gamma}(y,t) \end{cases} \tag{6}$$
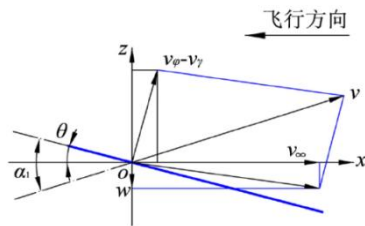

Figure 7: Kinematic model of the strip   Figure 8: Aerodynamic model of the strip
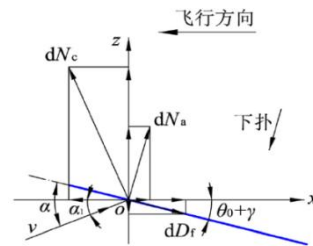
According to Rayner[5], the airflow forms an unsteady wake vortex behind the trailing edge of the wing and the underwash effect of these unsteady wake vortices cannot be ignored. Based on the traditional element theory, this paper takes the influence of the underwash effect into consideration. According to the theoretical analysis of the elliptical wing by Kuethe[6], the expression of the strip underwash speed is as follows.

$$w(t) = \frac{2(\alpha_0 + \theta(t))}{2 + \lambda(t)} v_\infty \tag{7}$$

α_0 is airfoil zero lift angle of attack, α_0 of flat wing type is $0°$. $\lambda(t)$ is the airfoil aspect ratio with time as a parameter variable. $\theta(t)$ is geometric angle of attack, which is equal to the sum of the airfoil mounting angle θ_0 and the twist angle $\gamma(y,t)$, $\theta(t) = \theta_0 + \gamma(t)$ （rad）. The velocity vector at the aerodynamic center of the strip is as follows.

$$V(t) = \left\{ \left[\sqrt{v_\varphi^2 + v_\gamma^2} \cos\theta(t) - w(t) \right]^2 + \left[\sqrt{v_\varphi^2 + v_\gamma^2} \sin\theta(t) + v_\infty \right]^2 \right\}^{\frac{1}{2}} \tag{8}$$

$$\lambda(t) = \frac{2b \cdot 2b}{2b \cdot c} = \frac{4b^2(t)}{S} = \frac{4\left[e_1 b \sin\theta_1(t) + e_2 b \sin\theta_2(t) + e_3 b\right]^2}{2\left[c \cdot e_1 b \sin\theta_1(t) + c \cdot e_2 b \sin\theta_2(t) + \frac{\pi}{4} c(e_3 b)\right]} \tag{9}$$

$$S = 2\left[c \cdot e_1 b \sin\theta_1(t) + c \cdot e_2 b \sin\theta_2(t) + \frac{\pi}{4} c(e_3 b)\right] \tag{10}$$

$$c_n(y) = 2\pi\alpha(t, \ y, \ k) \ , \quad k = \frac{\omega b(t)}{V(t)} \tag{11}$$

S is the wing area, as shown in equation (10). The lift coefficient and the reduction frequency are as shown in equation(11). The Jones' unsteady normal force coefficient method is used to correct the dynamic angle of attack and the following formula considers the underwash effect.

$$\alpha' = \frac{\lambda(t)}{2 + \lambda(t)}\left[F'(k)\alpha_1 + \frac{c(y)G'(k)}{2v_\infty k}\dot{\alpha}_1\right] - \frac{w(t)}{v_\infty} \tag{12}$$

In the above formula, k is the reduced frequency and ω is the angular frequency of the simple harmonic motion.

$$F'(k) = 1 - \frac{C_1 k^2}{k^2 + C_2^2}, \quad G'(k) = 1 - \frac{C_1 C_2 k}{k^2 + C_2^2}, \quad C_1 = \frac{0.5\lambda(t)}{2.32 + \lambda(t)}, \quad C_2 = 0.181 + \frac{0.772}{\lambda(t)} \tag{13}$$

3.2 Aerodynatic model of the tiny wing strip

Considering only the FWA's flying forward at a uniform speed state, according to the aerodynamic generation mechanism, the aerodynamic forces of the tiny strip can be divided into: cycloid lift dN_c, additional mass force dN_a and frictional resistance dD_f. This study is aimed at a flat flexible wing and the flapping amplitude and angle of attack are not large, so the influence of leading edge suction and differential pressure resistance is not considered. The aerodynamic model of the strip is shown in Figure 8.

（1）Cycloid lift is the main source of aerodynamic forces, which is produced by the amount of loop around the airfoil. The direction of the Cycloid lift is perpendicular to the resultant relative flow direction. The value of Cycloid lift can be obtained from the Kuta-Ruukovsky theorem by the following formula.

$$dN_c = \frac{1}{2}\rho V^2(t) c_n(y) c\, dy \ , \quad N_c = \int_0^{b(t)} \frac{1}{2}\rho V^2(t) c_n(y) c\, dy \tag{14}$$

（2）The additional mass force, which is the force acting on the airfoil during the fluttering of the virtual cylinder surrounding the strip. It is a non-loop force due to the relative motion of the airflow and the airfoil. V_N is the normal velocity at the midpoint of the strip.

$$dN_a = \frac{1}{4}\rho\pi c^2 \dot{V}_N(t)\, dy \tag{15}$$

$$V_N(t) = \left[v_\varphi(t) - w(t)\right]\cos\theta(t) + \left[2v_\gamma(y,t) + v_\infty\right]\sin\theta(t) \tag{16}$$

（3）The frictional resistance of the strip is as follows.

$$dD_f = \frac{1}{2}\rho V_T^2(t) C_{D_f} c\, dy \tag{17}$$

V_T is tangential velocity at the midpoint of the strip， C_{D_f} is frictional resistance coefficient.

$$V_T(t) = -\left[\nu_\varphi(t) - w(t) \right] \sin\theta(t) + \left[2\nu_{\gamma}(y,t) + v_\infty \right] \cos\theta(t) , \quad C_{D_f} = \frac{2 \times 1.328}{\sqrt{Re}} \tag{18}$$

The above three aerodynamic components are decomposed in the vertical and horizontal directions. Vertical aerodynamics and horizontal aerodynamics are as follows.

$$dF_L = dN_c \cos\alpha_1 + dN_a \cos\theta - dD_f \sin\theta \tag{19}$$

$$dF_T = dN_c \sin\alpha_1 - dN_a \sin\theta - dD_f \cos\theta \tag{20}$$

Integrate the above two equations along the wingspan direction.

$$\begin{cases} F_L(t) = 2\int_0^{b(t)} dF_L \\ F_T(t) = 2\int_0^{b(t)} dF_T \end{cases} \tag{21}$$

3.3 Aerodynamic solution and analysis

The kinematic model of FWA proposed in this paper includes four degrees of freedom (flutter, twist, in-plane folding and out-of-plane folding). The aerodynamic force of the airfoil is solved by the element theory method considering the underwash effect. Refer to Ramezani[7] for parameter setting and compare the wind tunnel measurement results in Ramezani[7] with the results of this paper. The results show that the variation trend of vertical aerodynamic force is basically the same. The average vertical aerodynamic force in five cycles is 1.0953N, the average wind tunnel measurement is 1N and the relative error is 9.53%. There are three wind tunnel measurement tests in Figure 9(a). The solid red line is used as a reference. The fluorescent blue solid line in Fig. 9(b) is the numerical solution of the vertical aerodynamic force.
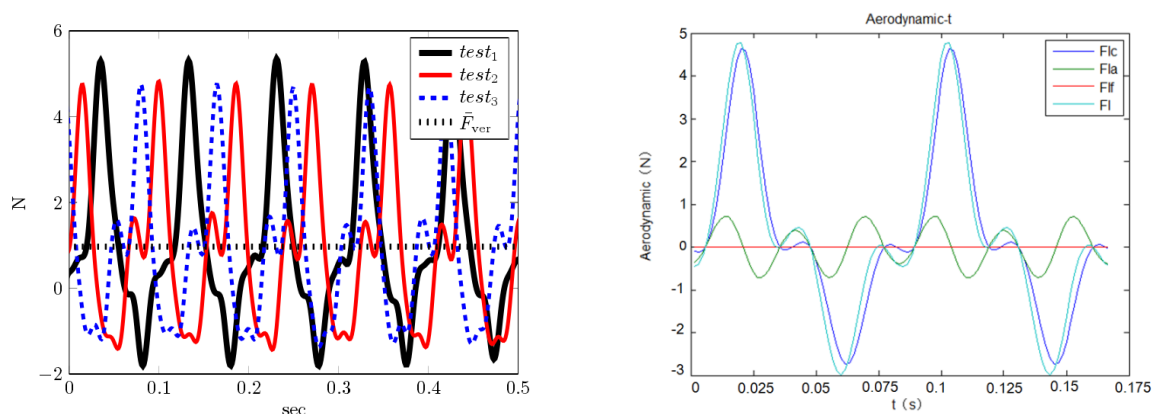
(a) Ramezani[7] Aerodynamic wind tunnel measurement results   (b) Aerodynamic results in this paper
Figure 9: Aerodynamic comparison of numerical solution and wind tunnel measurement results

4. Construction of dynamic model

4.1 Parameter values of the dytnamic model

This paper refers to Ramezani[7] for parameter setting. The Bat Bot column in the table below is the relevant parameters of the bat-like FWA in the literature. Rousettus aegyptiacus is the relevant parameter of the Egyptian fruit bat. The aerodynamic model is set using the Aerodynamics Model parameters, as shown in Table 1.

Table 1: Selection of parameters

Morphological parameters	Unit	Rousettus Aegyptiacus	Bat Bot	Aerodynamics Model
Aspect ratio	——	3.57	5.0	$\lambda(t)$
Frequency	Hz	10	10	10
Amplitude	deg	27.5	35	35
Mean wing span	m	0.469	0.6	0.6
Mean wing aera	m	0.0694	0.072	0.072
Mean wing chord	m	0.14	0.12	0.12
Total mass	kg	0.093	0.16	0.16
Body width	m	0.02	0.035	0.035
Humerus length	m	0.135	0.138	0.168
Radius length	m	0.145	0.168	0.168
Femur length	m	0.1	0.055	——

4.2 Longitudinal trim

In the case where the FWA is symmetrically straight and flat (height 20m, forward speed 7m/s), since the climb angle is zero, there is an angle of attack $\alpha = \theta$. The angular velocity around the rotation is zero. Longitudinal trim is as follows.

$$\begin{cases} X - mg\sin\theta = m[\dot{u} + qw - rv] = 0 \\ Z + mg\cos\theta\cos\phi = m[\dot{w} + pv - qu] = 0 \\ M = I_y\dot{q} - I_{zx}(r^2 - p^2) - (I_z - I_x)rp + h_B^r r = 0 \end{cases} \tag{22}$$

Substituting the aerodynamic numerical solution into the above equation. This paper only considers the longitudinal flight dynamics modeling and stability analysis, not include the transverse direction, the coupling of the longitudinal and transverse directions or the inertial force of the wing.

$$\begin{cases} X - mg\sin\theta = \dfrac{1}{2}\rho V_0^2 S C_x + T - mg\sin\alpha = 0 \\ Z + mg\cos\theta\cos\phi_0 = \dfrac{1}{2}\rho V_0^2 S C_z + mg\cos\alpha = 0 \\ M = \dfrac{1}{2}\rho V_0^2 S C_m \bar{c} = 0 \end{cases} \tag{23}$$

The FWA kinematics equations and dynamic equations are rewritten into a form of differential equations. The specific expressions are as follows.

$$\begin{cases} \dot{u} = -qw - g\sin\theta + \dfrac{F_L}{m} \\ \dot{w} = qu + g\cos\theta + \dfrac{F_T}{m} \\ \dot{q} = \dfrac{M_y}{I_y} \\ \dot{\theta} = q \\ \dot{x} = u\cos\theta + w\sin\theta \\ \dot{z} = u\sin\theta - w\cos\theta \end{cases} \tag{24}$$

7

Xuejiao Zhang, Yonghai Wang

4.3 Simulation results and analysis

(a) Vertical aerodynamics

(b) Horizontal aerodynamics

(c) Pitching moment

(d) Dynamic angle of attack
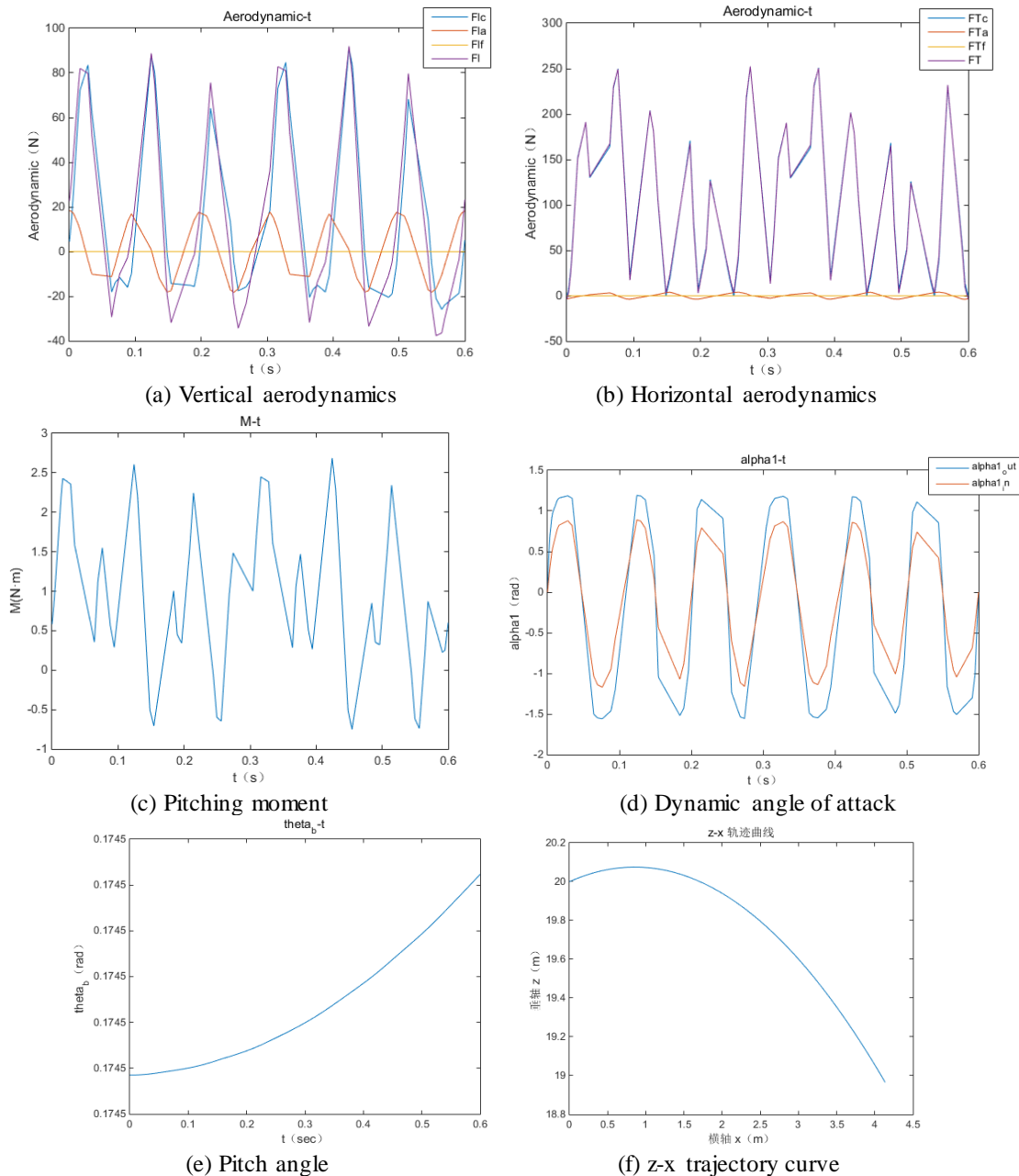
(e) Pitch angle

(f) z-x trajectory curve

Figure 10: Dynamic model simulation results

From Fig. 10, it can be concluded that: (1) the vertical/horizontal aerodynamic forces are composed of three aerodynamic components, namely, the cycloid lift, the additional mass force and frictional resistance. The cycloid lift is dominant. The aerodynamic model and the longitudinal flight dynamics model are coupled to obtain the average aerodynamic error in 6 cycle is no more than 15%. (2) The vertical aerodynamic value is positive during the wing flapping down, negative during flapping up. The horizontal aerodynamic is always positive during flapping up and down. (3) The dynamic angle of attack of the wing changes periodically, which is positive during flapping down and negative during flapping up. The dynamic angle of attack of the Handwing is larger than that of the Armwing. The value of the latter is about 62.5% of the former. (4) The response curve of the longitudinal pitching moment fluctuates drastically, whose magnitude of change is related to the weight of whole FWA. (5) When the weight of the FWA is large, the pitch angle is gently increased and the FWA is gently flying forward and falling. When the weight of the FWA is small (the actual mass of the Egyptian fruit bat is 0.16 kg), the response curve of the pitch angle fluctuates drastically and the FWA oscillates and falls.

5. Open-loop longitudinal stability

5.1 Floquet-Lyapunov Indirect method

The motion parameters of the FWA are time-varying, such as the velocity component u and w, the pitch rate q and the pitch angle θ. The aerodynamic and aerodynamic moments of the FWA vary periodically. We define the equilibrium state of FWA as the limit cycle state, which has the same flutter frequency as the FWA. The limit cycle of a dynamic system is a series of discrete periodic solutions of the dynamic model[8].

$$\dot{x} = f(x), \quad x \in R^n \tag{25}$$

$$x(t+T) = x(t), \quad \forall t \tag{26}$$

The periodicity of the limit cycle is represented by the following equation.

$$\begin{cases} \tilde{\mathbf{x}}_1 - \mathbf{x}_1 = 0 \\ \tilde{\mathbf{x}}_2 - \mathbf{x}_2 = 0 \\ \quad \vdots \\ \tilde{\mathbf{x}}_{m-1} - \mathbf{x}_{m-1} = 0 \\ \tilde{\mathbf{x}}_m - \mathbf{x}_m = 0 \end{cases} \tag{27}$$

While $\mathbf{x}_i = \mathbf{x}_i^{\neq}$, the above formula (27) is established by the Newton iteration method. The goal of the known integral trajectory $\tilde{\mathbf{x}}_i$ depends only on the estimated value $\mathbf{x}_{i-1}$ of the initial condition. The estimate $\mathbf{x}_i$ depends only on its own[9]. The iterative equation is as follows.

$$\begin{bmatrix} \dfrac{\partial \tilde{\mathbf{x}}_1}{\partial \tilde{\mathbf{x}}_0} & -I & 0 \cdots & 0 & 0 \\ \dfrac{\partial \tilde{\mathbf{x}}_2}{\partial \tilde{\mathbf{x}}_1} & -I \cdots & 0 & 0 \\ 0 & \ddots & \vdots & \vdots \\ \vdots & \vdots & \dfrac{\partial \tilde{\mathbf{x}}_m}{\partial \tilde{\mathbf{x}}_{m-1}} & -I \\ 0 & 0 & 0 \cdots & I \\ -I & 0 & 0 & I \end{bmatrix} \begin{bmatrix} \triangle \mathbf{x}_0 \\ \triangle \mathbf{x}_1 \\ \triangle \mathbf{x}_2 \\ \vdots \\ \triangle \mathbf{x}_{m-1} \\ \triangle \mathbf{x}_m \end{bmatrix} = - \begin{bmatrix} \tilde{\mathbf{x}}_1 - \mathbf{x}_1 \\ \tilde{\mathbf{x}}_2 - \mathbf{x}_2 \\ \vdots \\ \tilde{\mathbf{x}}_m - \mathbf{x}_m \\ \mathbf{x}_m - \mathbf{x}_0 \end{bmatrix} \tag{28}$$

A series of discrete points are interconnected to form a limit cycle and the Jacobian matrices are interconnected to form a state transition matrix.

$$\psi(t_m, t_{m-1}) \psi(t_{m-1}, t_{m-2}) \cdots \psi(t_2, t_1) \psi(t_1, t_0) = \psi(t_m, t_0) = M \tag{29}$$

M is a single-valued matrix of the entire loop. It should be noted that in the multiple shooting method, changing the order of multiplication greatly simplifies the calculation of the single-valued matrix.

5.2 Open-loop longitudinal stability analysis

The state transition matrix expression of the flight dynamics model of FWA is

$$\Phi(t_i,t_{i-1})=\begin{bmatrix} \dfrac{\partial \dot{u}_i}{\partial u_{i-1}} & \dfrac{\partial \dot{u}_i}{\partial w_{i-1}} & \dfrac{\partial \dot{u}_i}{\partial q_{i-1}} & \dfrac{\partial \dot{u}_i}{\partial \theta_{i-1}} \\[2mm] \dfrac{\partial \dot{w}_i}{\partial u_{i-1}} & \dfrac{\partial \dot{w}_i}{\partial w_{i-1}} & \dfrac{\partial \dot{w}_i}{\partial q_{i-1}} & \dfrac{\partial \dot{w}_i}{\partial \theta_{i-1}} \\[2mm] \dfrac{\partial \dot{q}_i}{\partial u_{i-1}} & \dfrac{\partial \dot{q}_i}{\partial w_{i-1}} & \dfrac{\partial \dot{q}_i}{\partial q_{i-1}} & \dfrac{\partial \dot{q}_i}{\partial \theta_{i-1}} \\[2mm] \dfrac{\partial \dot{\theta}_i}{\partial u_{i-1}} & \dfrac{\partial \dot{\theta}_i}{\partial w_{i-1}} & \dfrac{\partial \dot{\theta}_i}{\partial q_{i-1}} & \dfrac{\partial \dot{\theta}_i}{\partial \theta_{i-1}} \end{bmatrix} \qquad (30)$$

The single-valued matrix of the model in this paper is as follows

$$M=\begin{bmatrix} 1.0493 & -0.15826 & -0.28173 & -2.0693 \\ -0.36420 & 0.34023 & 0.62409 & 0.35153 \\ -0.33114 & 0.56531 & 1.1209 & 0.16127 \\ -0.038537 & 0.079968 & 0.21046 & 1.0099 \end{bmatrix} \qquad (31)$$

In this paper, the Floquet-Lyapunov indirect method is used to analyze the open-loop longitudinal stability. Refer to Ramezani[7] for parameter settings. The single-valued matrix of the FWA flight dynamics model in this paper has four eigenvalues. Their real parts are positive. Theoretically, the foldable flapping wing aircraft with uncontrolled control surface is longitudinally unstable. The specific conclusions are as follows.

1) $\lambda_1=1.8671$, which corresponds to this eigenvalue is $V_1=[-0.68\ \ 0.46\ 0.59\ 0.17]^{\mathrm{T}}$. $T_1=0.3712$

This eigenvalue corresponds to a short-period mode, the divergent oscillation frequency is relatively high, damping is relatively large, the attenuation is relatively fast and the doubling time is about 3.712 times the flapping period.

2) $\lambda_2=0.025945$, which corresponds to this eigenvalue is $V_2=[0.062\ \ 0.92\ -0.45\ 0.020]^{\mathrm{T}}, T_2=26.71$

This eigenvalue corresponds to the long-period mode (sink-floating mode), the divergent oscillation frequency is relatively low, and the damping is relatively small; the doubling time is about 267.1 times the flapping period.

3) $\lambda_{3,4}=0.65537\pm0.35657i$, $\upsilon_{3,4}=\left[0.87\ 0.063\pm0.15i, 0.45\pm0.21i, 0.054\mp0.17i\right]^{T}$ The doubling time is about 10.57 times the flapping period. $T_{3,4}=1.057$. Relative damping ratio is $\xi=0.34$. Natural frequency is $\omega_n=2.16$ rad/s. Settling time is $t_s=5.44$.

6. Closed-loop longitudinal stability.

A robust variable gain control method (LPV system with parameter dependent Lyapunov Function) is proposed. The solution of the linear matrix satisfying the LMI is found by the combination of the multi-cell vertices and the controller parameter matrix is obtained. The controller is substituted to obtain a simulation curve for a specific operating condition. A set of simulation curves for a given operating condition is obtained to obtain the closed-loop longitudinal stability of the FWA.

6.1 Control law design method for state feedback

The parameter relies on the feedback controller, that is, constructs a variable gain controller of the form (32) to stabilize the system[10].

$$u = K(\theta)x \tag{32}$$

The expression of the LPV system with parameter dependent Lyapunov Function is as follows:

$$\dot{x} = A(\theta)x + B(\theta)u \tag{33}$$

We substitute the state feedback controller (32) into the system (33) to get the closed-loop system expression as follows:

$$\dot{x} = A_{cl}(\theta)x , \quad A_{cl}(\theta) = \sum_{i=0}^{n}\theta_i A_i + \sum_{i=0}^{n}\sum_{j=0}^{n}\theta_i\theta_j B_i K_j \tag{34}$$

6.2 Linear variable parameter control system modeling

When the FWA's wings are folded, the area of the wing becomes smaller, the lift is reduced and the FWA will dive down. To ensure that the wing folding process is sufficiently stable, the controller is designed to control the variation value of vertical height and speed during the complete wing folding process. During the folding process of the wing, the deflection angle of the elevator is relatively large and the throttle change is relatively small. In this paper, the elevator yaw angle is used as a single control quantity and the throttle opening degree is automatically controlled. The structural design of the longitudinal stability control system during the FWA wing folding process is as follows.
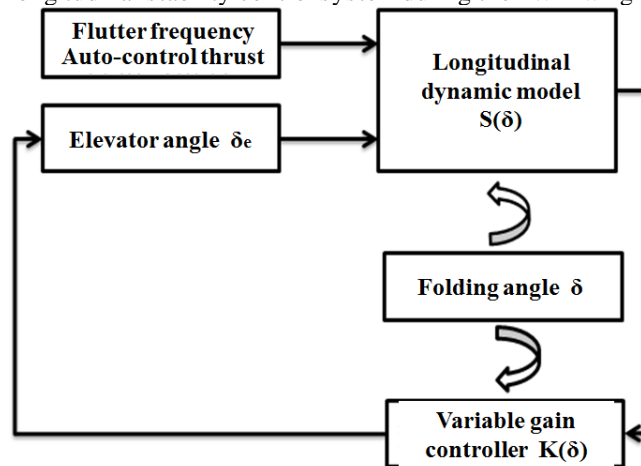

Figure 11: FWA longitudinal stability controller system structure diagram

The throttle opening is automatically controlled and the input is $U = \triangle\delta_e$. The variable parameter formula of the state space model is shown as Fig. 11 and as follows.

$$B = \begin{bmatrix} 0 \\ -0.0794 \\ 0 \\ -24.4081 \\ 0 \end{bmatrix} \tag{35}$$

Xuejiao Zhang, Yonghai Wang

We convert the state matrix A (containing the amount of folding angle variation δ) into a multicellular form.

$$A(\delta) = A_0 + \delta A_1$$

$$A_0 = \begin{bmatrix} -0.00913469 & 4.35174 & -9.80000 & 0 & 0 \\ -0.00105815 & -0.685638 & 0 & 1.00000 & 0 \\ 0 & 0 & 0 & 1.00000 & 0 \\ 0 & -12.2766 & 0 & -1.18765 & 0 \\ 0 & 133.200 & 133.200 & 0.00000 & 0 \end{bmatrix}$$ (36)

$$A_1 = \begin{bmatrix} 0.0000209667 & -0.0208140 & 0 & 0 & 0 \\ 0.00000401839 & 0.00277612 & 0 & 0 & 0 \\ 0 & 0 & 0 & 0 & 0 \\ 0 & -0.0262395 & 0 & 0 & 0 \\ 0 & 0 & 0 & 0 & 0 \end{bmatrix}$$ (37)

We get the linear matrix inequality equation as follows:

$$\begin{cases} \bar{P}_0 A_1^T + A_1 \bar{P}_0 + \bar{P}_1 A_0^T + A_0 \bar{P}_1 + \bar{K}_1^T B^T + B\bar{K}_1 - H_{01} - H_{01}^T \le 0 \\ \begin{bmatrix} \bar{P}_0 A_0^T + A_0 \bar{P}_0 + \bar{K}_0^T B_0^T + B_0 \bar{K}_0 & H_{01} \\ H_{01} & \bar{P}_1 A_1^T + A_1 \bar{P}_1 \end{bmatrix} < 0 \\ \bar{P}_1 < 0 \\ \bar{P}_0 > 0 \\ \bar{P}_0 + 60\bar{P}_1 > 0 \end{cases}$$ (38)

$$\bar{K}_0 = \begin{bmatrix} 0.00131770 & 0.0250496 & 0.0249432 & -0.0200463 & -0.00911153 \end{bmatrix}$$

$$\bar{K}_1 = \begin{bmatrix} 2.45090e\text{-}5 & 2.35268e\text{-}5 & -7.87043e\text{-}7 & 0.00803262 & 6.22689e\text{-}8 \end{bmatrix}$$

$$\bar{P}_0 = \begin{bmatrix} 0.00487249 & 3.35153e\text{-}5 & 6.94819e\text{-}5 & 0.000914532 & -0.0705040 \\ 3.35153e\text{-}5 & 8.37944e\text{-}5 & 9.12128e\text{-}5 & -0.00288618 & -0.000327499 \\ 6.94819e\text{-}5 & 9.12128e\text{-}5 & 0.000107913 & -0.00469284 & -0.00125407 \\ 0.000914532 & -0.00288618 & -0.00469284 & 0.606199 & -0.0167194 \\ -0.0705040 & -0.000327499 & -0.00125407 & -0.0167194 & 2.99864 \end{bmatrix}$$

$$\bar{P}_1 = \begin{bmatrix} -3.32256e\text{-}5 & 1.96775e\text{-}7 & 4.16878e\text{-}11 & -4.03713e\text{-}6 & 4.91056e\text{-}13 \\ 1.96775e\text{-}7 & -4.51999e\text{-}9 & 1.85487e\text{-}13 & 2.59725e\text{-}8 & 2.17777e\text{-}15 \\ 4.16878e\text{-}11 & 1.85487e\text{-}13 & -1.11447e\text{-}8 & -6.16219e\text{-}8 & -8.10024e\text{-}6 \\ -4.03713e\text{-}6 & 2.59725e\text{-}8 & -6.16219e\text{-}8 & -1.98406e\text{-}5 & 4.41899e\text{-}7 \\ 4.91056e\text{-}13 & 2.17777e\text{-}15 & -8.10024e\text{-}6 & 4.41899e\text{-}7 & -0.0133983 \end{bmatrix}$$ (39)

The numerical solution of the above four controller parameter matrices is substituted into equation (40).Controller systemcontains only an indeterminate fold angle δ. The numerical solution of the controller parameter matrix is substituted into the systemmodel and an attempt is made to apply robust stabilization controlling to the FWA.

$$K(\theta) = \left(\sum_{i=0}^{n} \theta_i \bar{K}_i \right) \left(\sum_{i=0}^{n} \theta_i \bar{P}_i \right)^{-1}$$ (40)

12

6.3 Controller simulation results and analysis

(a) Forward speed　　　　　　　　　　　　　　(b) Vertical height

(c) Dynamic angle of attack　　　　　　　　　　(d) Elevator angle

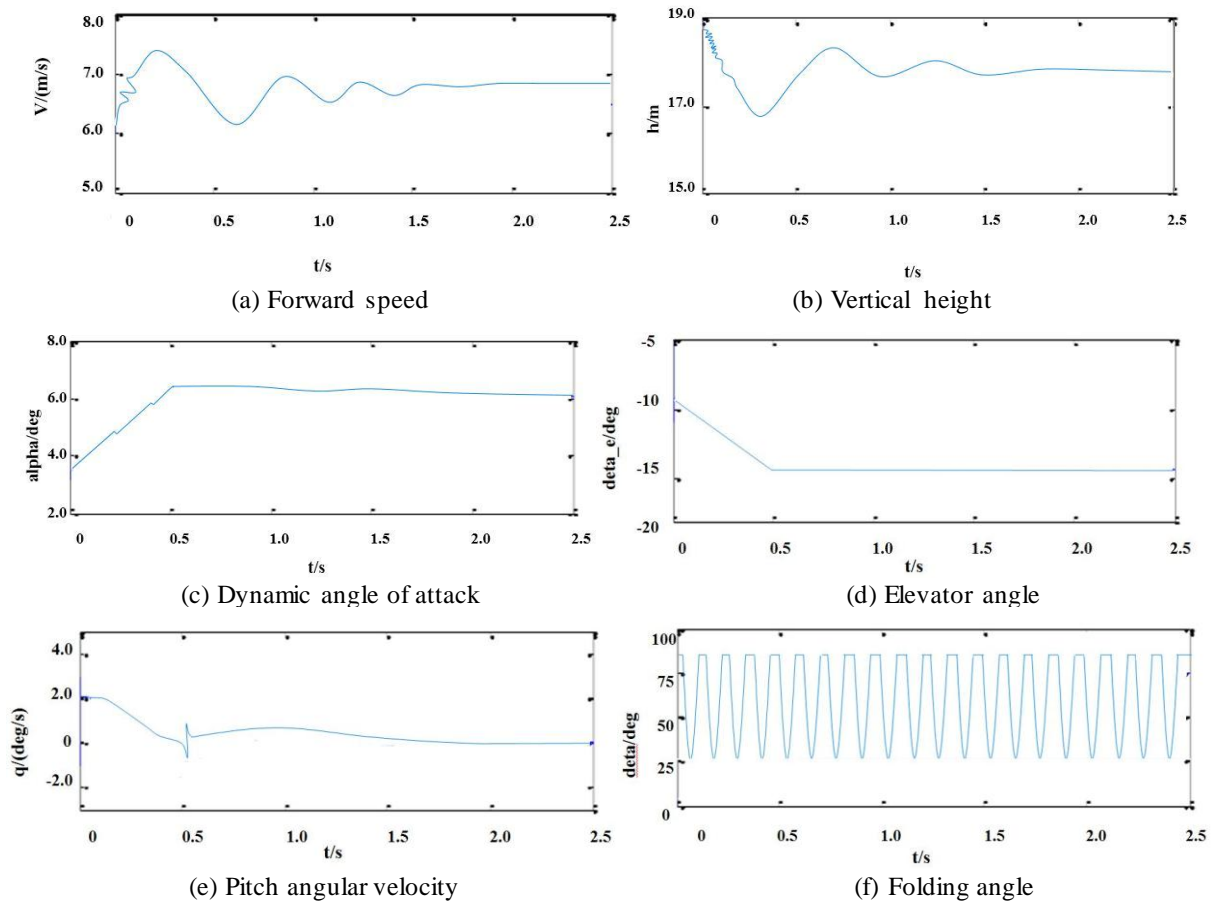(e) Pitch angular velocity　　　　　　　　　　　(f) Folding angle

Figure 12: FWA closed-loop simulation curve

The closed-loop longitudinal stability of FWA is studied by using robust variable gain control method (parameter dependent Lyapunov function). Firstly, the folding angle and the aerodynamic parameters are simplified and fitted to a large extent and the affine parameter dependence model is constructed. If the time-varying parameter is in a finite space, the affine parameter LPV model perform a multi-cell combination of the extreme values of the time-varying parameter. Solve the numerical solution of the controller parameter matrix that satisfies the LMI. The initial flight speed is 6m/s, the height is H=19m and the simulation time is from 0s to 2.5s, as shown in Figure 12.

The preliminary simulation results of closed-loop longitudinal stability are analyzed as follows:

1) The angle of attack increases by 2° from 0s to 0.5s and the flight of the aircraft decreases by 2m.

2) The pitch angular velocity curve fluctuates greatly. The amplitude of pitch angle and angle of attack both reach the maximum at 0.5s.

3) After 0.5s, under the action of the stabilization controller, the simulation curve gradually converges and basically stabilizes around 2s.

4) Theoretically, the robust variable gain control method (parameter dependent Lyapunov Function) is feasible for the closed-loop longitudinal stability control of the FWA flight dynamics model.

7. Conclusion

This paper studies the bat-like foldable FWA airfoil aerodynamic modeling problem. The accuracy of the aerodynamic modeling method is verified by comparing the aerodynamic numerical solution results with the bat wind tunnel observation experimental data. The flight dynamics model is constructed to obtain the time domain response curve of each motion parameter. On this basis, the longitudinal stability of the open-loop is analyzed. From the theoretical level, the feasibility of the closed-loop longitudinal stability control is preliminarily explored.

This paper ignores the influence of the wing inertial force during the process of FWA flight dynamics modeling. Subsequent research attempts to extend flight dynamics modeling to rolling direction and yaw direction. The closed-loop longitudinal stability study of FWA is based on the linear fitting of both wing folding angle and aerodynamic

force. Subsequent further studies can focus on high-order nonlinear fitting of the folding angle and aerodynamic forces, as well as different closed-loop control law designs.

References

[1] Khan Zaeem A,Agrawal Sunil K. Force and Moment Characterization of Flapping Wings for Micro Air Vehicle Application [C]// American Control Conference. 2005, June 8-10, Portland or USA: 1515-1520.
[2] Smith Michael J C,Wilkin Peter J,Williams March. The Advantages of an Unsteady Panel Method in Modelling the Aerodynamic Forces on Rigid Flapping Wings [J]. Journal of Experimental Biology (S0022-0949), 1996, 199(5): 1073-1083.
[3] Lasek M, Pietrucha J, Zlocka M, Sibilski K. Analogies between Rotary and Flapping Wings from Control Theory Point of View [C]//AIAA Atmospheric Flight Mechanics Conference and Exhibit, 2001, 6-9 August, Montreal, Canada: 1-9.
[4] Thielicke W, Stamhuis E J. The Influence of Wing Morphology on The Three-Dimensional Flow Patterns of A Flapping Wing at Bird Scale [J]. Journal of Fluid Mechanics, 2015, 768: 240-260.
[5] Rayner J.M.V. A Vortex Theory of Animal Flight. Part 2. The Forward Flight of Birds[J].Journal of Fluid Mechanics, 2006, 91(04):731-763.
[6] Kuethe A.M., Chow C.Y. The Finite Wing. Foundations of Aerodynamics[M]. 4th ed,John Wildy, New York, 1986:145-164.
[7] Ramezani A,Chung S J,Hutchinson S. A Biomimetic Robotic Platform to Study Flight Specializations of Bats[J]. Science Robotics 2, eaal2505,2017,46-59.
[8] John M. Dietl, Ephrahim Garcia. Stability in Ornithopter Longitudinal Flight Dynamics[J]. Journal of Guidance, Control, and Dynamics, 2008(4):1157-1162.
[9] Travin A, Shur M, Strelets M, et al. Physical and Numerical Upgrades in the Detached-Eddy Simulation of Complex Turbulent Flows[J]. Advances in Les of Complex Flows, 2002, 65:239-254.
[10] Felten F, Fautrelle Y, Terrail Y D, et al. Numerical modelling of electromagnetically-driven turbulent flows using LES methods[J]. Applied Mathematical Modelling, 2004, 28(1):15-27.